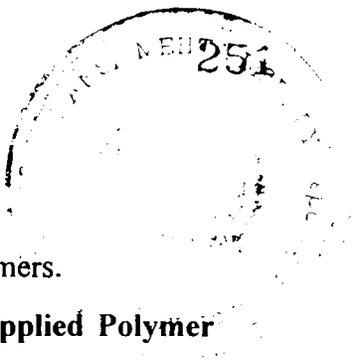

List of Publications :

1) Synthesis and Charaterization of Some Water-Soluble Polymers.
Anuradha Rangaraj, V. Vangani and A. K. Rakshit. **J. Applied Polymer Science,** 66, 45, ***1997.***

2) Polymer-Surfactant Interaction Studies in Aqueous System.
Anuradha Rangaraj and A. K. Rakshit. **Indian J. of Chemistry** 37A, 222, ***1998.***

Synthesis and Characterization of some Water Soluble Polymers

ANURADHA RANGARAJ, VEENA VAŅGANI, ANIMESH K. RAKSHIT

Department of Chemistry, Faculty of Science, M.S. University of Baroda, Baroda 390002, India

Received 7 June 1996; accepted 16 January 1997

ABSTRACT: Homopolymers and copolymers of acrylamide (AA) and acrylic acid (AAc) were synthesized by the free radical solution polymerization technique. Feed ratios of the monomers were 85 : 15 (w/w), 65 : 35 (w/w), and 50 : 50 (w/w) of acrylamide and acrylic acid, respectively, for synthesis of copolymers. All reactions were carried out in aqueous media, except for the synthesis of polyacrylic acid, where the medium was *n*-butanol. Hydrogen peroxide, potassium persulfate, and benzoyl peroxide were used as initiators. The copolymers were purified by removing homopolymers. The homopolymers and copolymers were characterized by infrared (IR), ^{13}C-nuclear magnetic resonance (NMR), ^{1}H-NMR, differential scanning calorimetry (DSC), thermogravimetric analysis (TGA), and viscosity measurements. The fusion temperature and the energy change for various phase transitions were obtained from DSC measurements. The activation energy values for various stages of decomposition were calculated from TGA. The activation parameters for the viscous flow (i.e., free energy, enthalpy, and entropy of activation) were evaluated from the viscosity measurements. Voluminosity and Simha shape factor were also calculated for different systems. Effects of various concentrations of electrolytes, $NaNO_3$, and $Al(NO_3)_3$ on viscosity behavior were studied.
 J Appl Polym Sci **66**: 45–56, 1997

Key words: homopolymer; copolymer; polyacrylic acid; polyacrylamide; characterization; synthesis

INTRODUCTION

Polyacrylamide and copolymers of acrylamide with other monomers have shown a number of properties leading to a variety of industrial applications. Of growing importance are those related to their use as water soluble viscosifiers and displacement fluids in enhanced oil recovery.[1] Polyacrylamide as such has a variety of applications due to its ability to flocculate solids in aqueous suspensions.[2] Acrylamide-based polyelectrolytes were found to reduce surface charges and enable the primary particles to coagulate.[3] Acrylic acid and its copolymers with acrylamide and other monomers are used in fields as varied as mining, textile manufacture, oil-well drilling, secondary oil recovery, and agricultural soil modification.[4] The solution properties of polyelectrolytes are rather unusual. A decrease in the viscosity of polyacrylamide solutions in the presence of mono and multivalent electrolytes (e.g., NaCl, $CaCl_2$, etc.) is well known.[5]

Different researchers in recent years have worked with polyacrylamide (PAA), polyacrylic acid (PAAc), and their copolymers. IR spectroscopy has been used to study the complexation of PAA with PAAc.[6] Copolymers of acrylamide with methyl acrylate,[7] and sodium acrylate[8] have been studied spectroscopically. Acrylamide-acrylic acid copolymers are being used as thickeners for improved performance in alkaline conditions.[9] A recent review discusses the properties and uses of copolymers of acrylamide with acrylic acid and various acrylates

Correspondence to: A. K. Rakshit.
Journal of Applied Polymer Science, Vol 66, 45–56 (1997)
 CCC 0021-8995/97/010045-12

in the petroleum industry.[10] The copolymerization of acrylamide and acrylic acid[11] has been studied recently with reference to amounts of initiator, temperature, pH, time, etc. Tercopolymerization of acrylic acid, acrylamide and *N*-[(4-decyl)phenyl] acrylamide has been reported.[12] Our interest in the synthesis and characterization of water soluble PAA, PAAc, and P(AA-AAc) copolymers arises because of our desire to study the interaction of these polymers with various ionic and nonionic surfactants, as both polymers and surfactants are present in these systems.

In this article we present the synthesis and characterization of polyacrylamide, polyacrylic acid and acrylic acid-acrylamide copolymers. The effect of $NaNO_3$ and $Al(NO_3)_3$ on the viscosity property of the aqueous solutions of the above-mentioned homo and copolymers are also discussed in detail.

EXPERIMENTAL

Acrylamide (Mitsubishi Chemicals Ltd.) and acrylic acid (National Chemical, Baroda) were used for polymerization without any prior purification. Potassium persulfate (Merck, India) and hydrogen peroxide (Glaxo, India, 30% w/v) were used as received. The solvents were freshly distilled prior to use.

Elemental analysis was done on a FISONS, EA 1108, C, H, N analyzer.

IR spectra of the films of the homopolymers and copolymers were recorded on a Shimadzu IR-408 spectrophotometer. The films were prepared by dissolving the polymers in water and pouring the solution over a pool of mercury. The films were obtained by vacuum evaporation of the solvent.

The NMR of the polymer solutions in D_2O were recorded on a Varian XL, 300 MHz, for PMR and 75 MHz for ^{13}C-NMR, at the RSIC, IIT, Bombay, India.

TGA was recorded on a Shimadzu thermal analyzer DT-30 B. The TGA analysis was done in the presence of air. DSC was recorded on a Mettler ME 4000.

Viscosity studies of different solutions were carried out with the help of an Ubbelohde viscometer, placed vertically in a thermostat, at all required temperatures (±0.05°C).

Polymerization of acrylamide, acrylic acid, and their copolymers, in various feed ratios, was carried out by the free radical solution polymerization technique[13] as described below.

Polyacrylamide was synthesized as follows: 20% (w/v) solution of acrylamide in water, in presence of 10 mL H_2O_2 (3% w/v) was taken in a three-necked flask, under nitrogen atmosphere. The reaction mixture was stirred at 82°C for a period of one-half hour. The three-necked flask was equipped with a water condenser and was placed in a thermostat maintained at the desired temperature. The reaction mixture after polymerization was poured into an excess of methanol to precipitate out the PAA. The PAA obtained was repeatedly washed with methanol and finally dried *in vacuo* before characterization.

Synthesis of PAAc was carried in nonaqueous medium: 40 g of acrylic acid in 160 g of *n*-butanol was taken in a three-necked flask. The reaction set up was similar to that used for synthesis of PAA. Benzoyl peroxide (0.4 g) was used as the initiator. The reaction mixture was stirred for a period of 5 h under a nitrogen atmosphere at 80°C. PAAc was obtained by pouring the reaction mixture into the nonsolvent, nonane. It was dried *in vacuo* before characterization.

Copolymerization of acrylic acid and acrylamide was carried out with different feed ratios of the two monomers.[14] The ratios chosen for study were 50 : 50, 65 : 35, and 85 : 15 (w/w) acrylamide and acrylic acid, respectively. The recipe for the synthesis of copolymer 85 : 15 (w/w) of acrylamide and acrylic acid (AA-AAc) was as follows: 17 g acrylamide, 3 g acrylic acid, and 0.14 g $K_2S_2O_8$ were taken in 180 mL of H_2O. The reaction was carried out under nitrogen atmosphere at 68°C for a period of 2.5 h. The reaction set-up remained the same as described in the earlier paragraph. The polymeric product was obtained by reprecipitation in methanol. The reprecipitated product was further purified by removal of the respective homopolymers. The homopolymer PAAc was soluble in dioxane. The product obtained on reprecipitation was treated with dioxane to remove PAAc. The product hence obtained was dissolved in a methanol-water mixture (50 : 50 v/v). The homopolymer PAA remained insoluble and was filtered out. The copolymer, which was soluble in the water-methanol mixture, was poured into an excess of pure methanol to reprecipitate the copolymer, which was thoroughly washed with methanol and finally dried *in vacuo*.

The reaction conditions were exactly the same for copolymers having acrylamide and acrylic acid in feed ratios 50 : 50 (w/w) and 65 : 35 (w/w). The reaction mixture was heated at 68°C for a period of 2.5 h under a nitrogen atmosphere. The polymeric product obtained was also purified to

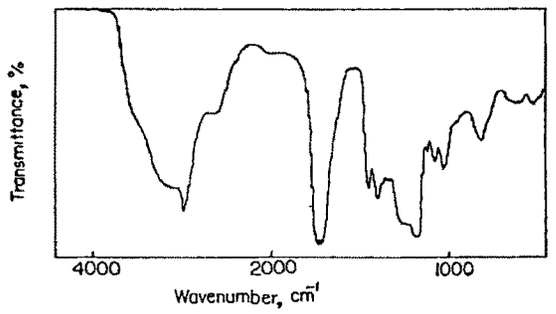

Figure 1 IR spectrum of PAAc.

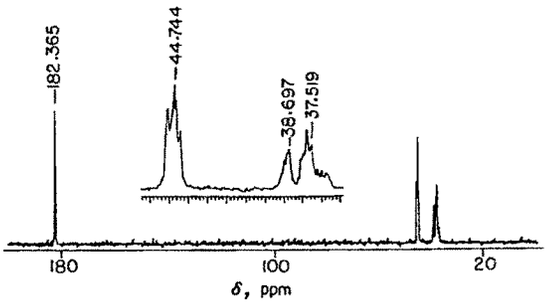

Figure 3 ^{13}C-NMR spectrum of PAA.

remove the respective homopolymers. The purification procedure was exactly the same as used for the previous copolymer.

RESULTS AND DISCUSSION

The IR spectrum of PAAc is shown in Figure 1. The broad absorption band due to the O—H bond present in the —COOH group was observed in the range of 3300–3500 cm^{-1}.[15] The C=O bond of carboxylic acid was observed at 1720 cm^{-1}. Two bands arising from C—O stretching and O—H bending appear in the spectrum. These are ~ 1320–1210 cm^{-1} and 1440–1395 cm^{-1}, respectively. Both of these bands involve some interaction between C—O stretching and in-plane C—O—H bending.[16] The IR spectra of AA-AAc copolymers show absorption bands typical of the constituent monomeric units and their relative intensity, depending on composition. The IR spectrum of AA-AAc copolymer (65 : 35) is shown in Figure 2. The C=O bond of the carbonamide group absorbs at 1650 cm^{-1}. The C—N stretching bond of primary amide was observed near 1400 cm^{-1}. PAA showed characteristic absorptions which agreed very well with those reported in the literature.[17,18]

Further evidence for the two comonomers incorporated was given by ^{13}C-NMR spectra of the copolymers. The ^{13}C-NMR spectra of PAA and copolymer AA-AAc (65 : 35) are given in Figures 3 and 4. The chemical shift values of PAA (Fig. 3) are in agreement with those reported earlier.[18–20] The methine carbon (—$CHCONH_2$) of the backbone resonates at 44.744 ppm and the backbone methylene carbon resonates between 36.768–38.971 ppm. The carbonyl carbon appeared as a sharp singlet at 182.365 ppm. In the case of AA-AAc copolymers (Fig. 4), an extra peak due to methine carbon (—CHCOOH) was observed at δ = 63.97 ppm.[21,22] The intensity of this peak increased with the increase in the amount of AAc incorporated. The carbonyl carbon of the —COOH group absorbs at δ = 178.399–179.345 ppm. The intensity of this peak also increased with the increase in AAc content. The absorptions of the backbone —CH_2 from both the monomers could not be distinguished from ^{13}C-NMR spectra. The proton spectra of homopolymers and copolymers (not shown) supported the ^{13}C-NMR spectra. The

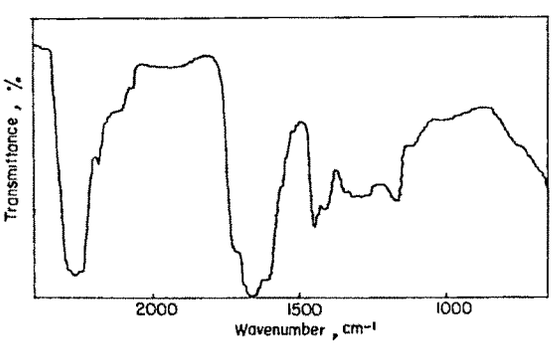

Figure 2 IR spectrum of copolymer AA-AAc (65 : 35).

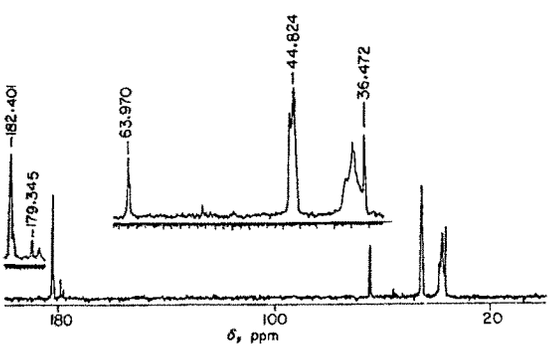

Figure 4 ^{13}C-NMR spectrum of copolymer AA-AAc (65 : 35)

Table I Composition of Acrylamide and Acrylic Acid in Feed and in Copolymers

Sample	Mole Fraction of AA in Feed (M_1)	Elemental Analysis N (%)	Mole Fraction of AA in Copolymer (ϕ_1)
AA-AAc (50 : 50)	0.504	8.66	0.44
AA-AAc (65 : 35)	0.653	10.16	0.52
AA-AAc (85 : 15)	0.852	14.86	0.76

methylene protons of PAA appeared as a broad peak at δ = 1.6–1.8 ppm.[22] The methine protons resonate at δ = 2.28 ppm. On incorporation of AAc, the extra peak at δ = 2.84 ppm was due to the backbone methine proton (—CHCOOH).

The feed ratios of various monomer mixtures, as well as the composition of the resulting copolymers obtained by elemental analysis, are summarized in Table I. The reactivity ratios of AA and AAc were estimated by the graphical method according to the Kelen–Tudos equation.[23]

$$\eta = r_1\xi - \frac{r_2(1 - \xi)}{\alpha} \qquad (1)$$

where r_1 and r_2 are the reactivity ratios relating to monomer 1 (acrylamide), and monomer 2 (acrylic acid), respectively. η, ξ, and α are mathematical functions of G and F as defined in Table II. On plotting η versus ξ, a linear plot was obtained. The intercepts at $\xi = 0$ and $\xi = 1$ gave $-r_2/\alpha$ and r_1, respectively. The values obtained for r_1 and r_2 are 0.427 and 0.945, respectively.

The reactivity ratios r_1 and r_2 were also determined by the Fineman–Ross method.[24] The following equation was used:

$$X(Y - 1)/Y = r_1(X^2/Y) - r_2 \qquad (2)$$

where $X = M_1/M_2$ and $Y = \phi_1/\phi_2$ (see Table II). On plotting $X(Y - 1)/Y$ against X^2/Y, a straight line was obtained whose slope was r_1 and the intercept yielded r_2. The values obtained for r_1 and r_2 by this method are 0.463 and 1.092 respectively. Several values of r_1 and r_2, depending on temperature and reaction conditions, are reported in the literature[25,26] for the same two monomers. As seen above, both the methods give similar values for r_1 and r_2.

The statistical distribution of monomer sequences, $M_1 - M_1$, $M_2 - M_2$, and $M_1 - M_2$ was calculated using the following relations[5,19]:

$$X = \phi_1 - 2\phi_1(1 - \phi_1)/[1 + [(2\phi_1 - 1)^2 + 4r_1r_2\phi_1(1 - \phi_1)]^{1/2}] \qquad (3)$$

$$Y = (1 - \phi_1) - 2\phi_1(1 - \phi_1)/[1 + [(2\phi_1 - 1)^2 + 4r_1r_2\phi_1(1 - \phi_1)]^{1/2}] \qquad (4)$$

Table II Kelen–Tudos Parameters

Sample	$X = \frac{M_1}{M_2}$	$Y = \frac{\phi_1}{\phi_2}$	$G = \frac{X(Y-1)}{Y}$	$F = \frac{X^2}{Y}$	$\xi = \frac{F}{\alpha + F}$	$\eta = \frac{G}{(\alpha + F)}$
AA-AAc (50 : 50)	1.01	0.80	−0.26	1.29	0.26	−0.05
AA-AAc (65 : 35)	1.88	1.08	0.14	3.29	0.47	0.019
AA-AAc (85 : 15)	5.75	3.10	3.90	10.64	0.74	0.27

$\alpha = \sqrt{F_{min} F_{max}} = 3.71$, M_2 is the mole fraction of acrylic acid in feed, ϕ_1 and ϕ_2 are the mole fractions of acrylamide and acrylic acid in the copolymer.

Table III Structural Data for the Copolymers of AA and AAc

Sample	Composition[a] (Mole fraction)		"Blockiness"[b] (Mole fraction)		Alternation[b] (Mole fraction)	Mean Sequence Length[c]		
	AA (ϕ_1)	AAc (ϕ_2)	AA-AA (X')	AAc-AAc (Y')	AA-AAc (Z')	μAA	μAAc	$\frac{\mu AA}{\mu AAc}$
AA-AAc (50 : 50)	0.44	0.56	0.14	0.260	0.600	1.3	2.2	0.6
AA-AAc (65 : 35)	0.52	0.48	0.215	0.175	0.610	1.5	1.9	0.8
AA-AAc (85 : 15)	0.76	0.24	0.552	0.032	0.417	2.4	1.3	1.8

[a] From elemental analysis.
[b] Statistically calculated using reactivity ratios (ref. 12).
[c] Using Kelen-Tudos reactivity ratio

$$Z = 4\phi_1(1 - \phi_1)/\{1 + [(2\phi_1 - 1)^2 + 4r_1r_2\phi_1(1 - \phi_1)]^{1/2}\} \quad (5)$$

where r_1 and r_2 are the reactivity ratios of AA and AAc, respectively. ϕ_1 is the mole fraction of acrylamide in the copolymer, obtained from elemental analysis. The mole fractions of 1 − 1, 2 − 2, and 1 − 2 sequences are designated by X', Y', and Z', respectively. Mean sequence lengths μ_{AA} and μ_{AAc} were calculated utilizing the relations:

$$\mu_{AA} = 1 + r_1[\phi_1]/[\phi_2] \quad (6)$$

$$\mu_{AAc} = 1 + r_2[\phi_2]/[\phi_1] \quad (7)$$

The intermonomer linkages and mean sequence length distributions for the AA-AAc copolymers are listed in Table III. For the series of AA-AAc copolymers, μ_{AA} varied from 1.3 at 0.44/0.56 mole ratio of AA/AAc in the copolymer to 2.4 with a 0.76/0.24 mole ratio. The calculated mole fraction of AA-AAc linkages in each copolymer was relatively high, indicating an alternating tendency.

TGA of PAA, PAAc, and copolymer AA-AAc (50 : 50) systems are given in Figure 5. The thermogram of the copolymer falls in between those of the corresponding homopolymers, implying a somewhat intermediate thermal stability. Two stage decomposition was observed in all cases, except for PAA. The first-stage decomposition of PAAc started at ~ 240°C. This is due to the formation of anhydride linkages. Similar values were reported earlier for PAAc.[27] Heating above 300–350°C results in rapid decomposition to monomer, carbon dioxide, and volatile hydrocarbons. TGA of PAA was three-staged, as observed before.[28] First, the loss of water, which is nonstoichiometric, occurred. This is followed by subsequent loss of ammonia and other gaseous products from the polyacrylonitrile structure formed during decomposition of polyacrylamide, and partly from the remaining polyacrylamide in the course of heating up to 600°C.[29]

The Ozawa method,[30] a dynamic analysis technique, was also used for the determination of activation energy. Thermograms were recorded at various heating rates of 10, 15, and 20 K min^{-1},

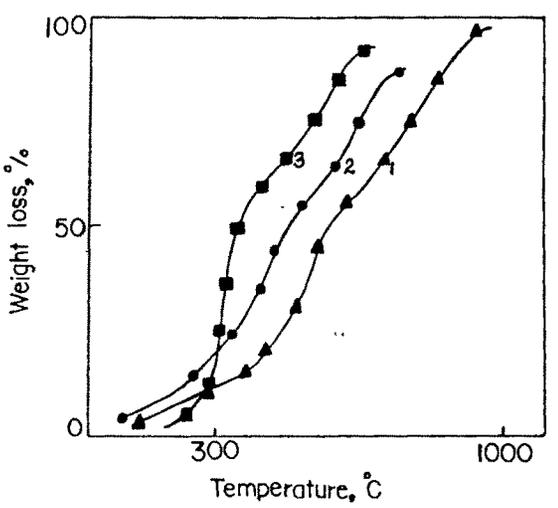

Figure 5 TG curves of (1) PAA, (2) copolymer AA-AAc (50 : 50), and (3) PAAc at heating rate of 10 K min^{-1} in air.

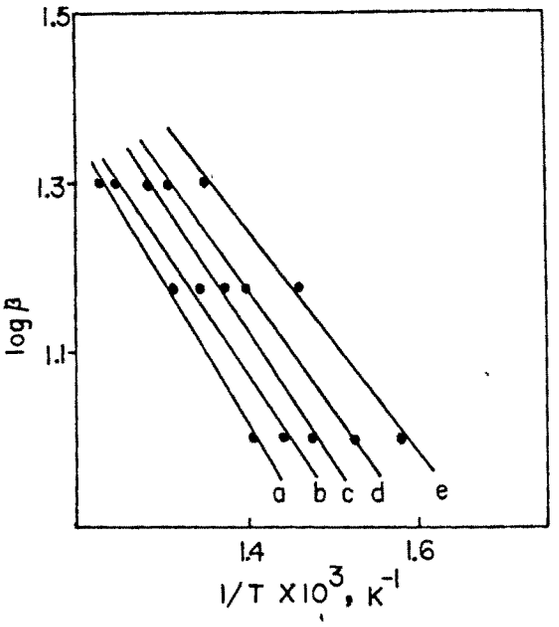

Figure 6 Plot of log β vs. $1/T$ for PAA. Values of $(1 - \alpha)$ are (a) 0.50; (b) 0.55; (c) 0.60; (d) 0.65, and (e) 0.70. β is the heating rate (K min^{-1}).

in air. The fraction of decomposition, α, was obtained by the following equation:

$$\alpha = (W_0 - W_t)/(W_0 - W_f) \qquad (8)$$

where W_0 is the initial weight of polymer, W_t is the weight of the polymer at temperature t, and W_f is the final weight. $(1 - \alpha)$ values were found for each heating rate from the TG curves; $(1 - \alpha)$ values obtained were plotted against $1/T$. According to Ozawa's method,[30] the plot of log β (where β is the heating rate) against the reciprocal of absolute temperature, for different values of $(1 - \alpha)$ is linear. The activation energy of decomposition was obtained from the slope of the above linear plot,[30] using the equation

$$\text{Slope} = -0.4567(E/R) \qquad (9)$$

The plot of log β versus $1/T$, for PAA, at different values of $(1 - \alpha)$ each differing by 0.05, is shown in Fig. 6. The activation energy values at different $(1 - \alpha)$ are given in Table IV. The activation energies of decomposition varied with $(1 - \alpha)$ and were not exactly constant. The activation energy of decomposition for PAA in a nitrogen atmosphere was 157.5 ± 1.71.[29] This indicates higher stability of PAA in a nitrogen atmosphere, as expected.

The activation energy associated with each stage of decomposition was also evaluated by the well-known Broido's method.[31–33] The equation used for the calculation of activation energy (E) was:

$$\ln \ln(1/Y) = (-E/R)(1/T) + \text{constant} \qquad (10)$$

where

$$Y = (W_t - W_\alpha)/(W_0 - W_\alpha) \qquad (11)$$

that is, Y is the fraction of the number of initial molecules not yet decomposed, W_t is the weight at any time t, W_α is the weight at infinite time (= zero), and W_0 is the initial weight. A plot of $\ln \ln(1/Y)$ versus $1/T$ [eq. (10)] gives an excellent approximation to a straight line over a range of $0.999 > Y > 0.001$. The slope is related to the activation energy. Representative plots are shown in Figure 7. The values for activation energy of decomposition are listed in Table V.

DSC curves for PAAc, PAA, and copolymer AA-AAc (85 : 15) are shown in Figures 8–10. Values of glass transition temperature (T_g) reported for PAAc in the literature are 106°C,[34] 130°C,[35] and 180°C.[36] The T_g of PAAc increases with increasing anhydride concentration, which occurs primarily by intramolecular reactions. Decarboxylation also occurs simultaneously with water elimination, but at a much slower rate.[37] DSC of PAAc (Fig. 8) shows a T_g at 116°C and the enthalpy change associated with it was 60.5 J g^{-1}. Melting temper-

Table IV The Activation Energies of Decomposition of Various Homopolymers and Copolymers

Polymer Sample	Activation Energy, E (kJ mol^{-1}) $(1 - \alpha)^n$			
PAA	30.4 (0.50)	28.0 (0.55)	28.1 (0.60)	24.9 (0.65)
AA-AAc (85 : 15)	83.9 (0.35)	85.1 (0.45)	82.1 (0.50)	83.0 (0.55)
AA-AAc (65 : 35)	84.5 (0.30)	81.8 (0.35)	84.5 (0.40)	78.4 (0.45)
PAAc	57.8 (0.40)	54.8 (0.45)	47.7 (0.50)	45.7 (0.55)

(Ozawa method, see text).
[a] Values of $(1 - \alpha)$ are given in parentheses.

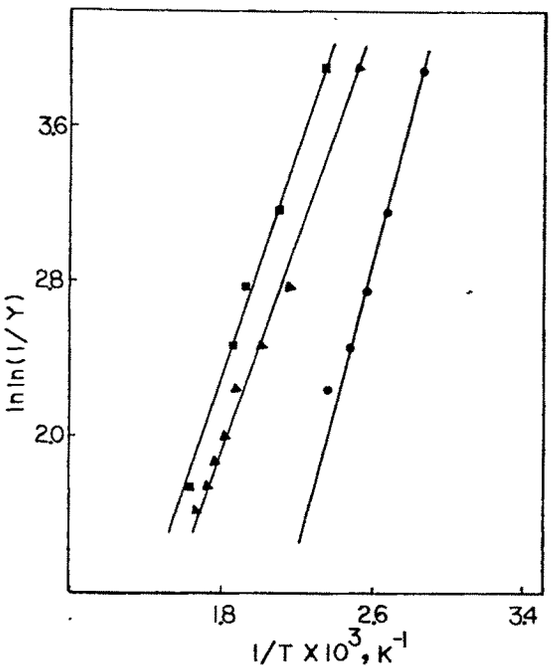

Figure 7 Plot of ln ln(1/*Y*) vs. 1/*T* for (●) PAA, (▲) AA-AAc (85 : 15), and (■) PAAc.

ature, T_m, of PAAc was 236°C and the enthalpy change associated with it was 486 J g^{-1}.[38] The fusion temperature and the energy change associated with the respective phase transitions are also listed in Table V. T_g of PAA (Fig. 9) was observed at 84.8°C and the onset of softening temperature occurred at ~ 190°C. Reported values were 153°C and 210°C, respectively.[39] AA-AAc copolymers showed an enhancement in T_g (Fig. 10) due to specific interactions between acrylamide and acrylic acid moieties.

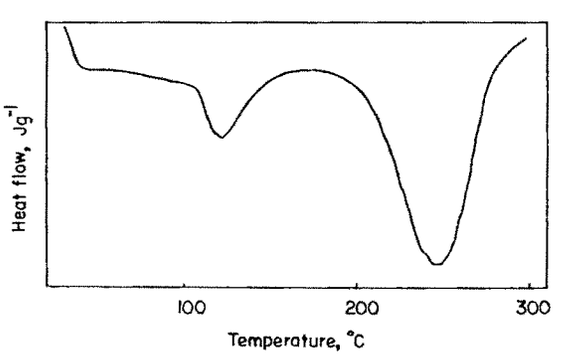

Figure 8 DSC curve of PAAc.

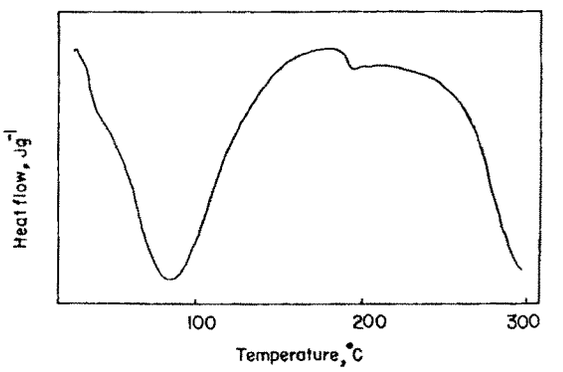

Figure 9 DSC curve of PAA.

The viscosity of solutions of PAA and copolymers AA-AAc (85 : 15), AA-AAc (65 : 35), and AA-AAc (50 : 50) was studied at different temperatures of 35, 40, and 45°C. The study was done in aqueous medium and in the presence of various concentrations of different electrolytes. Intrinsic viscosity was calculated using the following equations (Huggins & Kraemer):

$$\eta_{sp}/C = [\eta] + K'[\eta]^2C \quad (12)$$

$$\ln \eta_r/C = [\eta] - K''[\eta]^2C \quad (13)$$

where K' and K'' are constants for a given polymer/solvent/temperature system. For many linear flexible polymer systems, K' often indicates the measure of the solvent power; the poorer the solvent, the higher the value of K'. The $K' - K''$ values were found to be ~ 0.5, as expected.[40-42] Intrinsic viscosities of various systems at different temperature and some representative values of $K' - K''$ are given in Table VI. Some representa-

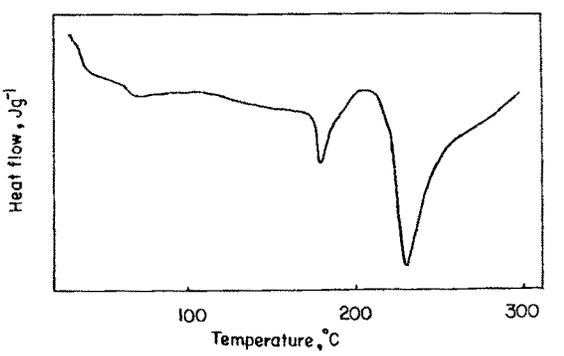

Figure 10 DSC curve of AA-AAc (85 : 15).

Table V Activation Energy of Decomposition, Fusion Temperature, and Enthalpy Change Values for Different Systems

Polymer Systems	Activation Energy (E)[a] (kJ mol^{-1})		Phase Transition Temperature (°C)	Enthalpy Change (J g^{-1})
	First Stage	Second Stage		
PAA	25.6	22.9	84.8	461.8
PAAc	8.9	2.9	a) 116.1 b) 236.1	a) 60.5 b) 486.1
AA-AAc (85 : 15)	19.1	34.8	a) 178.4 b) 228.8	a) 26.8 b) 218.1
AA-AAc (65 : 35)	17.7	36.1	a) 173.6 b) 226.1	a) 1.2 b) 108.5
AA-AAc (50 : 50)	20.3	20.7	a) 168.7 b) 228.4	a) 1.7 b) 67.6

[a] Calculated using Broidós method at a heating rate of 10 K min^{-1}, in air.

tive plots are shown in Fig. 11. The variation of $[\eta]$ with temperature depended on the salt concentration. $[\eta]$ of PAA in H_2O and in presence of lower concentrations of electrolytes [$NaNO_3$ and $Al(NO_3)_3$] showed a decrease with increase in temperature. Other systems showed an increase in $[\eta]$ with increase in temperature. The decrease in $[\eta]$ with increasing temperature indicates a decrease in hydrodynamic volume of polymer molecules. This is due to conformational and solvent association changes with increasing temperature.[43-45] Increase in temperature of a polymer solution generates two antagonistic effects.[43-45] First, increase in temperature generally leads to an increase in solvent power, i.e., solubility of the polymer in a solvent increases. This results in uncoiling of the polymer chains, leading to increase in $[\eta]$ with temperature. Second, increase in temperature may lower the rotational barrier, thereby enhancing the degree of rotation about a skeletal bond, forcing the molecular chains to assume a more compact coiled configuration. This leads to a decrease in $[\eta]$ with increase in temperature. The decrease in $[\eta]$ with increase in tem-

Table VI Intrinsic Viscosities of Various Polymer Systems at Different Temperatures in Aqueous Solutions

Polymer Systems/Solvent	Intrinsic Viscosity $[\eta]$ (dl g^{-1})			K'-K'' (40°C)
	35°C	40°C	45°C	
PAA/H_2O	2.98	2.91	2.62	0.51
PAA/0.05M $NaNO_3$	3.85	3.68	3.40	0.51
PAA/0.3M $NaNO_3$	3.87	3.67	3.58	0.50
PAA/0.5M $NaNO_3$	3.75	3.91	3.94	0.50
PAA/0.1M $Al(NO_3)_3$	4.00	3.74	3.56	0.49
PAA/0.3 M $Al(NO_3)_3$	3.97	4.04	4.53	0.50
PAA/0.5M $Al(NO_3)_3$	4.10	4.19	4.23	0.50
AA-AAc (65 : 35)/0.05M $NaNO_3$	1.52	1.62	1.74	0.49
AA-AAc (65 : 35)/0.1M $NaNO_3$	1.52	1.54	1.66	0.52
AA-AAc (65 : 35)/0.5M $NaNO_3$	1.52	1.53	1.58	0.48
AA-AAc (85 : 15)/0.3M $NaNO_3$	2.60	2.77	3.07	0.50
AA-AAc (85 : 15)/0.5M $NaNO_3$	2.36	2.73	2.92	0.50

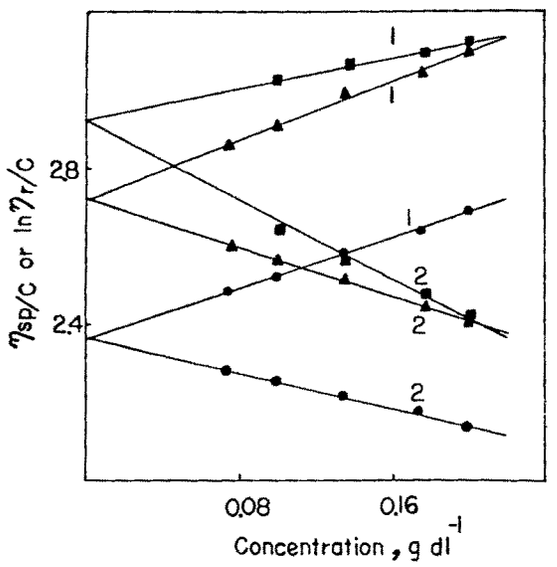

Figure 11 Typical plot of (1) η_{sp}/C and (2) ln η_r/C versus concentration for AA-AAc (85 : 15) at (●) 35°C, (▲) 40°C, and (■) 45°C in 0.5*M* aqueous $NaNO_3$.

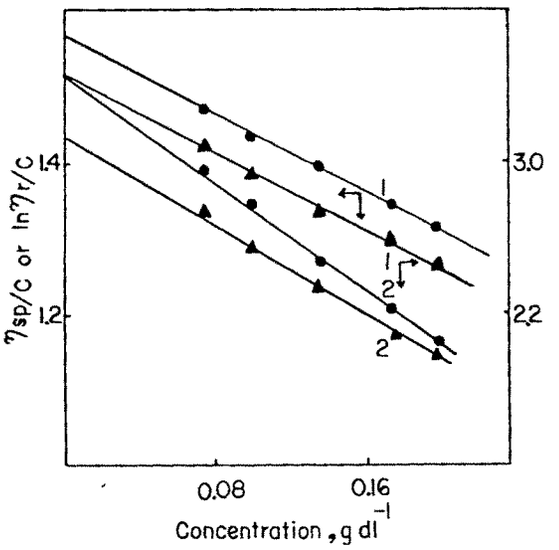

Figure 13 Plot of (1) η_{sp}/C and (2) ln η_r/C vs. concentration for (●) AA-AAc (50 : 50)/0.5*M* $NaNO_3$ at 45°C, and (▲) AA-AAc (50 : 50)/H_2O at 35°C

perature for various acrylamide-based copolymers was observed earlier.[5] On the other hand, polyelectrolytes like PAAc show an increase in [η] with increasing temperature.[46]

The effect of different concentrations of $NaNO_3$ on the viscosity behavior of PAA is different from that on the viscosity behavior of AA-AAc copolymers. [η] of PAA shows a maximum when plotted against the ionic strength of $NaNO_3$ (Fig. 12). This behavior for acrylamide-based copolymers was observed earlier.[5]

[η] of AA-AAc copolymer (65 : 35) varied linearly with reciprocal square root of ionic strength, i.e., $I^{-1/2}$ (Fig. 12). This behavior was observed for polyelectrolytes by a number of workers.[19,47-49]

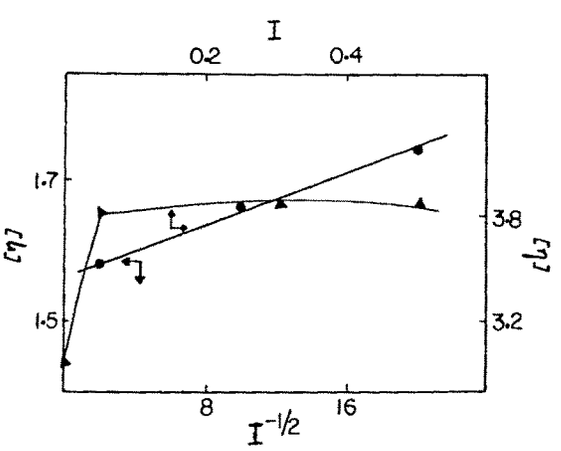

Figure 12 Plot of (●) $I^{1/2}$ vs [η] for AA-AAc (65 . 35)/$NaNO_3$ at 40°C, and (▲) I against [η] for PAA/$NaNO_3$ at 35°C.

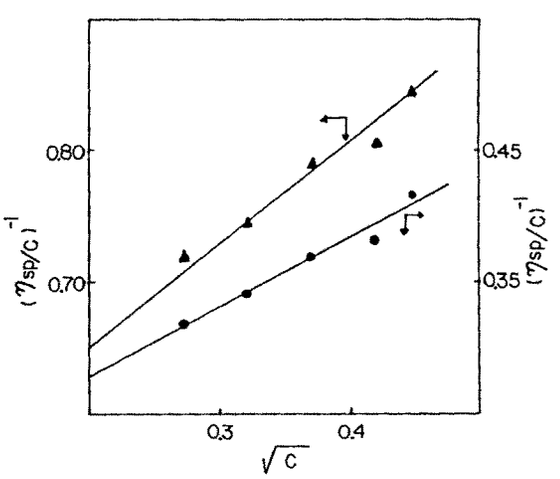

Figure 14 Plot of $(\eta_{sp}/C)^{-1}$ vs $(C)^{1/2}$ for (●) AA-AAc (50 . 50)/H_2O at 35°C and (▲) AA-AAc (50 . 50)/0.5*M* $NaNO_3$ at 40°C.

Table VII Voluminosity of Various Polymers at Different Temperatures

	Voluminosity (V_E)		
Polymer Systems/Solvent	35°C	40°C	45°C
PAA/H_2O	1.16	1.17	1.04
PAA/0.05*M* $NaNO_3$	1.48	1.45	1.34
PAA/0.3*M* $NaNO_3$	1.49	1.44	1.41
PAA/0.5*M* $NaNO_3$	1.46	1.48	1.53
PAA/0.1*M* $Al(NO_3)_3$	1.50	1.45	1.40
PAA/0.3*M* $Al(NO_3)_3$	1.51	1.54	1.55
PAA/0.5*M* $Al(NO_3)_3$	1.59	1.60	1.64
AA-AAc (65 : 35)/0.05*M* $NaNO_3$	0.57	0.61	0.64
AA-AAc (65 : 35)/0.1*M* $NaNO_3$	0.59	0.60	0.65
AA-AAc (65 : 35)/0.5*M* $NaNO_3$	0.58	0.59	0.63
AA-AAc (85 : 15)/0.3*M* $NaNO_3$	1.01	1.06	1.14
AA-AAc (85 : 15)/0.5*M* $NaNO_3$	0.90	1.09	1.12

This indicates that copolymers, having acrylic acid as a comonomer, act as polyelectrolytes in aqueous media. There is an electrical double layer at the solid–liquid interface (i.e., at the polyion–solvent interface). The double layer thickness at the polyion–solvent interface decreases with the addition of electrolyte. Hence, there is less overlapping of the double layers and consequently less viscosity with increase in the concentration of the salt.

The viscosities of AA-AAc (50 : 50), AA-AAc (65 : 35), and AA-AAc (85 : 15) in water, like other polyelectrolytes, showed a unique dependence on concentration. η_{sp}/C for the above-mentioned copolymers in water increases with dilution, contrary to the behavior of nonionic polymers. Representative plots are shown in Figure 13. As the solution is diluted, the polymer molecules no longer fill all of the space and intervening regions extract some of the mobile ions. Net charges develop in the domains of the polymer molecules, causing them to expand. As this process continues with further dilution, the expansive force increases. At high dilutions polymer molecules lose most of their mobile ions and are extended virtually to their maximum length.[50] This leads to high values of η_{sp}/C. Such data can be satisfactorily handled through the use of the empirical relation

$$\eta_{sp}/C = A/(1 + BC^{1/2}) \qquad (14)$$

where A and B are constants. Straight lines were obtained on plotting $(\eta_{sp}/C)^{-1}$ against $C^{1/2}$ (Fig. 14).[50] Addition of electrolyte suppresses the loss

Table VIII Shape Factor ν at Various Temperatures

	Shape Factor ν		
Polymer Systems/Solvent	35°C	40°C	45°C
PAA/H_2O	2.6	2.5	2.5
PAA/0.05*M* $NaNO_3$	2.6	2.6	2.5
PAA/0.3*M* $NaNO_3$	2.6	2.6	2.5
PAA/0.5*M* $NaNO_3$	2.6	2.6	2.5
PAA/0.1*M* $Al(NO_3)_3$	2.6	2.5	2.5
PAA/0.3*M* $Al(NO_3)_3$	2.6	2.5	2.5
PAA/0.5*M* $Al(NO_3)_3$	2.6	2.6	2.6
AA-AAc (65 : 35)/0.05*M* $NaNO_3$	2.6	2.6	2.6
AA-AAc (65 : 35)/0.1*M* $NaNO_3$	2.5	2.6	2.5
AA-AAc (65 : 35)/0.5*M* $NaNO_3$	2.6	2.6	2.5
AA-AAc (85 : 15)/0.3*M* $NaNO_3$	2.6	2.6	2.6
AA-AAc (85 : 15)/0.5*M* $NaNO_3$	2.5	2.5	2.6

Table IX Viscosity Activation Parameters at Infinite Dilution

Polymer Systems/Solvent	$\Delta H^{\ddagger 0}_{vis}$ (kJ mol^{-1})	$\Delta S^{\ddagger 0}_{vis}$ (JK^{-1} mol^{-1})	$\Delta G^{\ddagger 0}_{vis}$ (kJ mol^{-1}) 303 K
PAA/H_2O	15.9	38	4.5
PAA/0.05*M* $NaNO_3$	12.0	25	4.4
PAA/0.3*M* $NaNO_3$	16.8	40	4.5
PAA/0.5*M* $NaNO_3$	15.3	35	4.5
PAA/0.1*M* $Al(NO_3)_3$	22.5	58	5.0
PAA/0.3*M* $Al(NO_3)_3$	14.7	31	5.3
PAA/0.5*M* $Al(NO_3)_3$	14.8	35	4.3
AA-AAc (65 : 35)/0.05*M* $NaNO_3$	11.2	22	4.5
AA-AAc (65 : 35)/0.1*M* $NaNO_3$	21.4	55	4.7
AA-AAc (65 : 35)/0.5*M* $NaNO_3$	8.8	15	4.3
AA-AAc (85 : 15)/0.3*M* $NaNO_3$	16.2	39	4.4
AA-AAc (85 : 15)/0.5*M* $NaNO_3$	15.3	36	4.4

of mobile ions, hence the rise in η_{sp}/C at low concentrations was eliminated and the conformity with Huggins' equation was restored.

The relative viscosity data at different concentrations were used for the calculation of voluminosity (V_E) of polymer solutions at a given temperature.[40–42] V_E was obtained by plotting Y against concentration C (g ml^{-1}) where

$$Y = (\eta_r^{0.5} - 1)/C(1.35\eta_r^{0.5} - 0.1) \quad (15)$$

The straight line then obtained was extrapolated to $C = 0$ and the intercept yielded V_E. The values are listed in Table VII. The shape factor ν was calculated from the equation

$$[\eta] = \nu \cdot V_E \quad (16)$$

The shape factor gives an idea about the shape of macromolecules in solution.[51] Values of shape factor obtained for various systems are cited in Table VIII. All values were ~ 2.5, suggesting spherical conformations for the macromolecules in solution[52] both in presence and absence of electrolytes. Moreover, ν values were found to be independent of temperature (varying between 2.5 and 2.6), indicating that the minor axis varies by ~ 1%.

Various activation parameters of the viscous flow were evaluated using the Frenkel–Eyring equation[52]

$$\eta = Nh/V \exp \Delta G^{\ddagger}_{vis}/RT \quad (17)$$

where V is the molar volume of the solvent, N is the Avogadro number, h is the Planck's constant, R is the gas constant, T is the temperature, and $\Delta G^{\ddagger}_{vis}$ is the free energy of activation for the viscous flow. Equation (17) can be rewritten as

$$\ln(\eta V/Nh) = \Delta G^{\ddagger}_{vis}/RT = \Delta H^{\ddagger}_{vis}/RT - \Delta S^{\ddagger}_{vis}/R \quad (18)$$

where $\Delta H^{\ddagger}_{vis}$ and $\Delta S^{\ddagger}_{vis}$ are the enthalpy and entropy of activation for the viscous flow.[40–42] $\ln(\eta V/Nh)$, when plotted against T^{-1}, yields a linear graph, with slope and intercept giving $\Delta H^{\ddagger}_{vis}$ and $\Delta S^{\ddagger}_{vis}$, respectively. On plotting $\Delta H^{\ddagger}_{vis}$ and $\Delta S^{\ddagger}_{vis}$ values against concentration of polymer and extrapolating to $C = 0$, $\Delta H^{\ddagger 0}_{vis}$ and $\Delta S^{\ddagger 0}_{vis}$ values were obtained, respectively. $\Delta G^{\ddagger 0}_{vis}$ values were then computed by the well-known thermodynamic relation:

$$\Delta G^{\ddagger 0}_{vis} = \Delta H^{\ddagger 0}_{vis} - T\Delta S^{\ddagger 0}_{vis} \quad (19)$$

All activation parameters obtained at infinite dilution are given in Table 9. Positive values for $\Delta G^{\ddagger 0}_{vis}$, $\Delta H^{\ddagger 0}_{vis}$, and $\Delta S^{\ddagger 0}_{vis}$ were obtained for all systems. $\Delta G^{\ddagger 0}_{vis}$ remained almost constant for all systems studied. The $\Delta H^{\ddagger 0}_{vis}$ and $\Delta S^{\ddagger 0}_{vis}$ values vary with electrolyte and also with electrolyte concentration, but no regularity in the variations were noted.

Interestingly, on plotting $\Delta H^{\ddagger 0}_{vis}$ vs. $\Delta S^{\ddagger 0}_{vis}$ for all systems, a linear plot was obtained. The slope of the plot yielded a temperature of 312 K. Thus, at the temperature of 312 K, free energy of activation for the viscous flow becomes independent of the entropic forces and is solely governed by the enthalpic forces.

Thanks are due to IUC-DAEF, Indore, for financial assistance. Thanks are also due to the Research Laboratory of Sun Pharmaceuticals, Baroda, for DSC measurements and for nitrogen estimation.

REFERENCES

1. N. J. Bikales, Ed., *Water Soluble Polymers,* Plenum Press, New York, 1973.
2. F. Halverson and H. P. Panzer, in *Encyclopaedia of Chemical Technology,* Vol. 10, M. Grayson, Ed., Wiley, New York, 1980.
3. R. C. Schulz, in *Encyclopaedia of Polymer Science and Technology,* Vol. 1, J. I. Kroschwitz, Ed., Wiley, New York, 1985.
4. J. W. Brietebach and J. W. Kauffman, *Makromol. Chem.,* **175,** 2597 (1974).
5. C. L. McCormick and G. S. Chen, *J. Polym. Sci.,* **22,** 3649, 3633 (1984).
6. M. A. Moharram, L. S. Balloomal, and H. M. El-Gendy, *J. Appl. Polym. Sci.,* **59,** 987 (1996).
7. J. Yong and R. H. Huang, CA 124 : 56838a (1996).
8. Y. Morishima, T. Sato, and M. Kamachi, *Macromolecules,* **29,** 3960 (1996).
9. A. Tonson and M. I. William F, CA, 124: 147182 y (1996).
10. K. C. Taylor, E. D. Nasr, and A. Hisham, *J. Pet. Sci. Engg.,* **12,** 9 (1994).
11. Y. Zhao, J. Shen, and W. Li, CA 122: 188269 j (1995).
12. K. D. Branham, D. L. Danis, J. C. Middleton, and C. L. McCormick, *Polymer,* **35,** 4429 (1994)
13. T. J. Suen, A. M. Schiller, and W. H. Russel, in *Polymerization and Polycondensation Processes,* No. 34, N. A. J. Platzer, Ed., *Advances in Chemistry Series,* American Chemical Society, Washington, D.C., 1962.
14. S. H. Pinner, *J. Polym. Sci.,* **10,** 379 (1953).
15. W. M. Kulicke and H. H. Horl, *Colloid Polym. Sci.,* **263,** 530 (1985).
16. R. M. Silverstien, R. G. Bessler, and T. C. Morrill, *Spectrometric Identification of Organic Compounds,* 4th ed. Wiley, New York, 1981.
17. H. C. Haas and R. L. MacDonald, *J. Appl. Polym. Sci.,* **16,** 1972 (1972).
18. C. L. McCormick, G. S. Chen, and B. H. Hutchinson, *J. Appl. Polym. Sci.,* **27,** 3103 (1982).
19. C L. McCormick and K. P. Blackmon, *Polymer,* **27,** 1971 (1986).
20. S. J. Igarshi, *Polym. Sci., Polym. Lett. Ed.,* **1,** 359 (1963).
21. P. Bajaj, M Goyal, and R. B Chavan, *J. Appl. Polym Sci.,* **53,** 1771 (1994).
22. F. Candau, Z. Zekhnini, F. Heatley, and E. Franta, *Colloid Polym. Sci.,* **264,** 676 (1986).
23. T. Kelen and F. Tudos, *J. Macromol. Sci. Chem.,* **9,** 1 (1975).
24. M. Fineman and S. Ross, *J. Polym. Sci.,* **V,** 259 (1950).
25. G. Smets and A. M. Hesbain, *J. Polym. Sci.,* **XL,** 217 (1959).
26. J. Brandrup and E. H. Immergut, Eds., 2nd ed., *Polymer Handbook,* Wiley, New York, 1975.
27. D. H. Grand and N. Grassie, *Polymer,* **1,** 125 (1960).
28. L. M. Minsk, C. K. Chik, G. N. Meyer, and W. O. Kenyon, *J. Polym. Sci., Polym. Chem. Ed.,* **12,** 133 (1974).
29. M. Tutas, M. Saglam, M. Yuksel, and C. Guler, *Thermochim. Acta,* **111,** 121 (1987).
30. T. Ozawa, *J. Therm. Anal.,* **2,** 301 (1970).
31. A. Broido, *J. Polym. Sci.,* **7,** 1761 (1969).
32. R. Patel, K. C. Patel, B. N. Mankad, and R. D. Patel, *Proc. Indian Acad. Sci., (Chemical Science),* **89,** 561 (1980).
33. R. Joseph, S. Devi, and A. K. Rakshit, *J. Appl. Polym. Sci.,* **50,** 173 (1993).
34. L. J. T. Huges and D. B. Fordyce, *J. Polym. Sci.,* **22,** 509 (1956).
35. A. Odajima, A. E. Woodward, and J. A. Sauem, *J. Polym. Sci.,* **55,** 181 (1961).
36. H. L. Greenwald and L. S. Luskin, in *Handbook of Water Soluble Gums and Resins,* R. L. Davidson, Ed., McGraw–Hill, New York, 1980.
37. A. Eisenberg and T. Yokoyama, *J. Polym. Sci.,* **7,** 1717 (1969).
38. K. H. Illers, *Z. Kolloid,* **190,** 16 (1963).
39. M. L. Miller, *Can. J. Chem.,* **36,** 309 (1958).
40. E. A. Collins, J. Bares, and F. W. Billmeyer, *Experiments in Polymer Science,* 1st ed., Wiley, New York, 1970
41. V. Vangani and A. K. Rakshit, *J. Appl. Polym. Sci.,* **45,** 1165 (1992).
42. R. Joseph, S. Devi, and A. K. Rakshit, *Polym. Int.,* **26,** 89 (1991).
43. V. Vangani and A. K. Rakshit, *J. Appl. Polym. Sci.,* **60,** 1005 (1996).
44. G. M. Patel, N. K. Patel, and S. Kansara, *Polym. Int.,* **35,** 83 (1994).
45. A. K. M. Assaduzzaman, A. K. Rakshit, and S. Devi, *J. Appl. Polym. Sci.,* **47,** 1813 (1993).
46. A. Silberberg, J. Eliassaf, and A. Katchalsky, *J. Polym. Sci.,* **23,** 259 (1957).
47. I. Noda, T. T. Suge, and M. Nagasawa, *J. Phys. Chem.,* **74,** 710 (1970).
48. D. T. F. Pals and J. J. Hermans, *Rec. Trav. Chim.,* **71,** 433 (1952).
49. P. J. Flory, *J. Chem. Phys.,* **21,** 162 (1953).
50. P. J. Flory, *Principles of Polymer Chemistry,* 1st ed., Cornell University Press, New York, 1953.
51. H. H. Kohler and J. Strand, *J. Phys. Chem.,* **24,** 7628 (1990).
52. G. V. Vinogradov and A. Ya. Malkin, *Rheology of Polymers,* Mir Publishers, Moscow, 1980.

Indian Journal of Chemistry
Vol. 37A, March 1998, pp.222 - 227

Polymer-surfactant interaction studies in aqueous system

Anuradha Rangaraj & Animesh Kumar Rakshit*
Department of Chemistry, Faculty of Science, M S University of Baroda, Baroda 390 002, India

Received 4 February 1997; revised 26 November 1997

Polymer-surfactant interaction studies by surface tension, conductance, and viscosity measurements at various temperatures have been carried out between the nonionic polymer polyacrylamide ((PAA) and cationic surfactant cetyl trimethylammonium bromide (CTAB). The critical aggregation concentration (CAC) and polymer saturation point (PSP) have been computed and are found to decrease with increase in temperature. The effect of the increase in polymer concentration on CAC & PSP has been determined. The degree of ionization 'α', of the polymer-surfactant complex is computed which is found to increase with increase in temperature. The thermodynamic quantities associated with the PSP are computed

Polymer-surfactant (PS) interaction, which is akin to protein- surfactant interaction, has attracted much attention owing to their industrial applications e.g. in paints,, coatings,, cosmetics, tertiary oil recovery etc. as well as in biological systems[1,2]. The PS interaction has been studied by various methods[3-5]. All these studies indicate that polymers interact with surfactants by inducing micellization of surfactants on the polymer chain and after polymer gets saturated with the micelles, the excess surfactants form free micelles[6]. These polymer bound micelles have higher solubilizing power as well as viscosity in comparison to individual polymer or micelle[1].

In general it has been observed that the neutral polymers interact with anionic surfactants and show little or no tendency to interact with cationic or nonionic surfactants[7]. However, neutral polymers with some hydrophobicity and surface activity show significant interaction with cationic surfactants[8,9].

In this paper we present the results of a system containing polyacrylamide, a widely used neutral polymer and cationic surfactant cetyl trimethylammonium bromide (CTAB). The surface as well as thermodynamic properties associated with the system have been computed. The viscosity of the system was also determined.

Materials and Methods

Polyacrylamide was prepared by free-radical polymerization technique using hydrogen peroxide as an initiator. characterization of polymer was done by IR, NMR, TGA, elemental analysis and other methods[10]. The viscosity average molecular wt. was 6.76 x 10^5. Cetyl trimethylammonium bromide (CTAB) [Trizma Chemicals, India] was recrystallised from acetone - methanol (75 : 25) (v/v) mixture and dried before use. No minimum was observed in the surface tension-concentration profile of CTAB solution and the critical micelle concentration of CTAB was 0.93 m*M* at 30°C (lit. value[11] 0.90 m*M*). Triply distilled water was used. Critical micelle concentration was obtained by surface tension (γ) measurement using a du Noüy tensiometer (S C Dey & Co., Calcutta). Measurements were made at 30, 35, 40 and 45°c. The temperature was maintained constant by circulating thermostated water through a jacketed vessel containing the solution. Concentration of the solution was varied by adding aliquots of concentrated stock solution to the known volume of the solution in the jacketed vessel with the help of a microsyringe.

The two break points of γ versus log *C* plots (*C* is the concentration (M) of surfactant solution) are critical aggregation concentration (CAC) and polymer saturation point (PSP). Conductance measurements at various temperatures were carried out by Mullard conductivity bridge having a dip type cell with a cell constant of 0.6645 cm^{-1}. Plots of conductance versus concentration of surfactant give break points which were CAC and PSP. Viscosity measurements at 30, 35, 40 & 45°C were carried out using a 4 armed Ubbelohde viscometer.

Results and Discussion

The conductance versus surfactant concentration plots (Fig.1) exhibit three linear regions, below the CAC, between the CAC and PSP, where micelle like aggregates develop and above the PSP where co-existence of dynamic equilibrium of surfactant saturated polymer and regular micelles[6] occur. The CAC decreases with rise in temperature (0.83 m*M* at 30°C to 0.40 at 45°C) but not much variation is observed with change in polymer concentration. It is generally accepted that the polymer-surfactant binding starts at CAC[4]. This binding is similar to micellization but occurs at a relatively lower concentration of surfactant. With the increase in surfactant concentration, a second transition known as CMC of the polymer-surfactant complex or the polymer-saturation point (PSP) is obtained[12]. Table 1 gives PSP values for PAA-CTAB by both surface-tension and conductance measurements. Both methods give similar values. It is seen that as temperature increases, the PSP value decreases indicating the saturation of the polymer at lower concentration. this is because the micelles are present as a necklace[4] in the polymer chain where the neutral polymer molecule decreases the ion-ion repulsion. Increase in temperature does not have such effect on this necklace but the aggregation number of the surfactant decreases and hence PSP decreases. It is known that the CMC increases with increase in polymer concentration[13] in solution. This is because as polymer concentration increases, more binding sites are available, hence more surfactant is needed for micellization. That is PSP in-

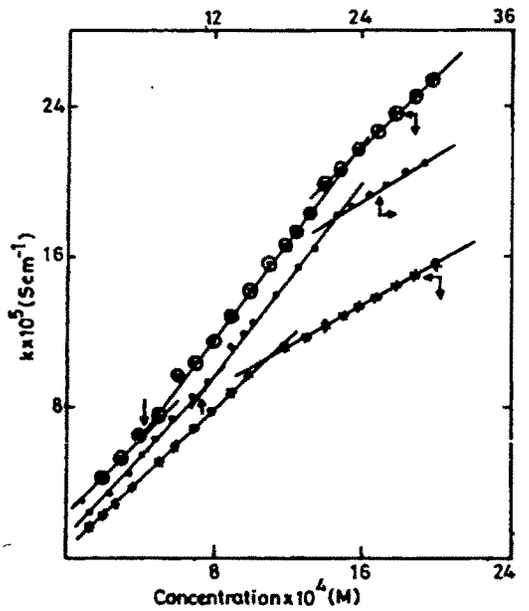

Fig.1 — Plot of specific conductance K vs. concentration at 30°C of CTAB solution in absence and presence of PAA.
✱ CTAB; ● with 0.001% PAA; ⊙ with 0.003% PAA

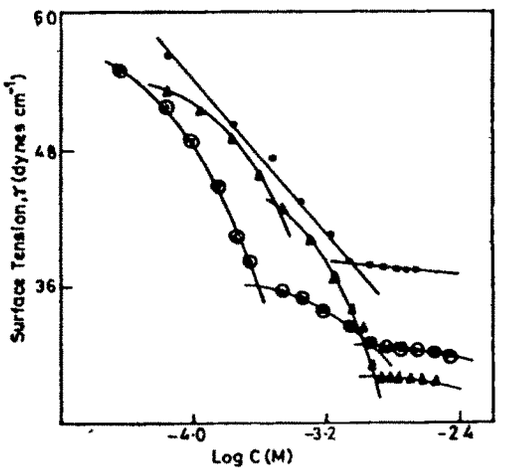

Fig.2 — Plot of surface tension (γ) vs. log concentration (log *C*) for ● pure CTAB at 30°C, ▲ 0.00001% PAA 35°C, ⊙ 0 003% PAA at 45°C

Table 1 — Polymer saturation point (PSP) values by surface- tension and conductance measurements

Polymer concentration % (w/v)	PSP from Surface Tension (mM)				PSP from Conductance (mM)			
	30°C	35°C	40°C	45°C	30°C	35°C	40°C	45°C
0.00001	0.82	0.67	0.40m	0.34	0.82	0.65	0.44	0.34
0.0001	1.78	1.24	1.10	0.98	1.70	1.43	1.19	1.10
0.001	1.92	1.39	1.10	0.66	1.94	1.47	1.09	0.67
0.002	2.40	1.91	1.46	1.07	2.40	1.90	1.46	1.14
0.003	2.40	2.18	1.49	1.05	2.42	2.18	1.49	1.05

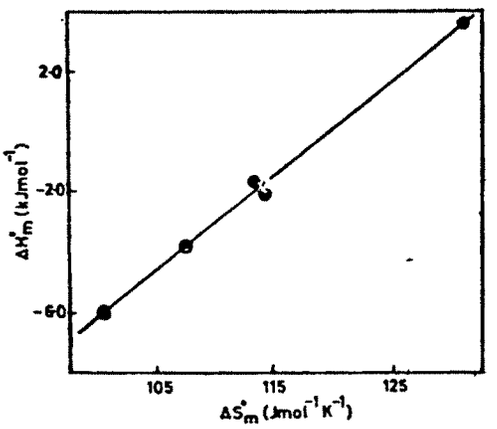

Fig.3 — The plot of ΔH°_m vs. ΔS°_m

creases with increase in polymer concentration. In Fig.2, representative surface tension γ - log C plots are shown.

The degree of ionization, 'α' of an ionic micelle depends on the method of determination[14]. It is computed from the ratio of slopes[15] of the conductance - concentration plot below and above the PSP. Zana *et al* [15] obtained α' to be 65% and 85% for PEO-SDS and PVP-SDS complexes respectively which are comparable with our values of 60-80%. With these 'α' values, the free energy of micellization (ΔG°_m)at PSP was calculated using the relation[16].

$$\Delta G^\circ_m = (2 - \alpha)\, RT \ln C_{PSP}$$

where C_{PSP} is in the mole fraction scale. The calculated values at 35°C are given in Table 2. The parameter ΔG°_m at other temperatures was also computed and found to become more negative with increase in temperature. A linear ΔG°_m - T plot (corr. coeff. 0.989-0.999) was used to compute ΔS°_m and ΔH_m (Table 2). The Δ°_m values fall around 100 J/mol/K for all systems and ΔH°_m values are negative indicating exothermic interaction. However, at 0.003% polymer concentration, the interaction seems to be endothermic and repeated experiments reproduced the value. On plotting enthalpy vs entropy changes at various polymer concentrations a linear correlation was obtained (Fig.3). At around ΔS°_m values of 120 J $mol^{-1}K^{-1}$ the ΔH°_m becomes zero. In this condition $\Delta G^\circ_m = - T\Delta S^\circ_m$. This indicates that the polymer surfactant interaction in this condition depends only upon the entropy change. Such enthalpy-entropy compensation effect was observed earlier in many physico-chemical processes[17,18]. The slope of the straight line was 312 K (in water, the suggested value is 270-294 K[18]). At 312 K, the micellization process is totally independent of structural changes in the system and depends on ethalpic forces[17-19].

From the surface-tension data, surface excess concentration (Γ) at the liquid-air interface was calculated using the Gibbs adsorption equation

$$\Gamma = - (1/2.303\ n\ RT)\ (d\gamma/d \log C)$$

where n is the number of particles per molecule of the surfactant whose concentration varies with surfactant bulk phase concentration[20]. In case of CTAB, n is 2, R is the gas constant (8.314 J) and T is the absolute temperature ($d\gamma/d$ log C) was computed at log C = - 3.5 where C is in molar scale. Γ increases with rise in temperature. However, change in Γ is irregular with change in polymer concentration. The increase in surface excess values with increase in temperature (Table 2) may be due to polymer induced partial shifting of interacting surfactant molecules from the bulk to the surface. Minimum area per molecule A_{min} was also calculated from surface-tension data, using the relationship,

$$A_{min} = (10^{14} / N.\Gamma)\ nm^2$$

Table 2 — Standard free energy, entropy and enthalpy of formation of SPS and surface excess concentration (Γ) in polyacrylamide-CTAB solutions

Polymer conc % (w/v)	$-\Delta G^\circ_m$ (kJ mol^{-1}) (35°C)	ΔH°_m (kJ mol^{-1})	ΔS°_m (kJ mol^{-1} K^{-1})	$10^{10}\ \Gamma$ mol cm^{-2}			
				30°C	35°C	40°C	45°C
0.00001	37.2	-2.1	114	0.30	0.50	0.80	1 11
0.0001	35.9	-1.1	114	0.25	0.57	0.62	0.89
0.001	37.0	-3.8	108	0.25	0.50	0.56	0.58
0.002	36.9	-5.9	101	0.23	0.28	0.31	0 36
0.003	36.8	3.4	131	0.43	0.49	0 57	0.70

Table 3 -- Intrinsic viscositty [η], voluminosity v_E and shape factor (υ)for polyacrylamide CTAB systems at different temperatures

Surfactant conc % (w/v)	Intrinsic viscosity [η] (dl/g)				V_E 35°C (dlg^{-1})	ν 35°C
	30°C	35°C	40°C	45°C		
0 00	-	2.98	2 91	2 62	1 16	2 6
0 01	3.04	3.19	3.09	3 06	1 19	2.7
0 05	3 15	3.33	3.18	3.14	1 21	2 7
0 01	3.30	3.47	3 23	3 20	1 28	2.7

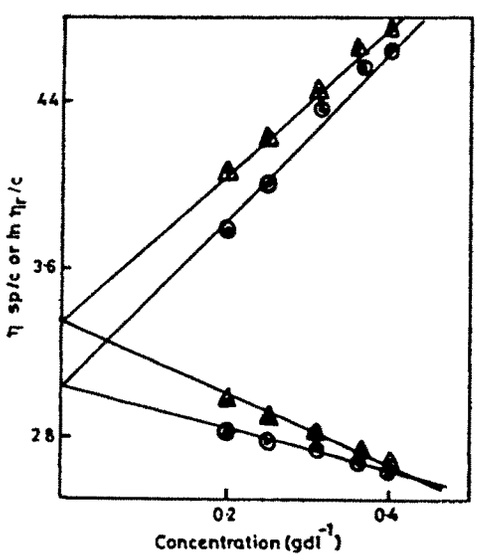

Fig.4 — Representative plots of η_{sp}/C and ln η_r/C vs. concentration of PAA for ⊙-0.01% CTAB- PAA at 30°C
▲-0 05% CTAB-PAA at 35°C.

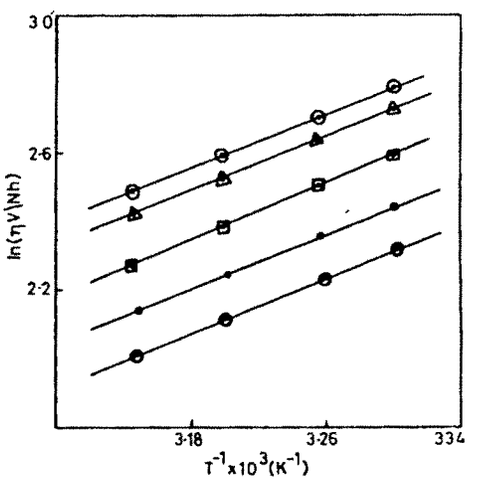

Fig 5 — Plot of ln (ηV/Nh), vs T^{-1} for 0 01% (CTAB + PAA) system at different PAA concentrations PAA values are·
⊙ 0 4%. ▲-0 3636. ⊡-0 3076%. ●-0.25% ⊖ 0 2%

where N is the Avagadro's number. Values of Γ are given in Table 2 and hence A_{min} can easily be calculated.

Viscosity of the polymer-surfactant solutions was also determined. Intrinsic viscosity of the polymer (Fig.4) was determined in the presence of various amounts of surfactants. It was observed that the intrinsic viscosity of the PAA increased as the concentration of CTAB increased in solution (Table 3). The intrinsic viscosity-temperature profile shows a maximum ~ 35°C for all concentrations of surfactants studied. This indicates that as temperature increases, solvent power increases and solubility of polymer increases resulting in the uncoiling of the polymer chains, providing interaction possibility leading to an increase in [η]. But as temperature further rises, the kinetic energy helps in the lowering of the rotational barrier and thereby enhancing the degree of rotation about a skeletal bond allowing the molecular chains to assume a more compact coiled configuration[21]. This leads to decrease in [η] with increase in temperature.

Various activation parameters for the viscous flow were evaluated using Frenkel-Eyring equation[21]

$$\ln (\eta V/Nh) = \Delta G^{\ddagger}_{vis}/RT = \Delta H^{\ddagger}_{vis}/RT - \Delta S^{\ddagger}_{vis}/R$$

where $\Delta H^{\ddagger}_{vis}$ and $\Delta S^{\ddagger}_{vis}$ are the enthalpy and entropy of activation for the viscous flow and V, N, h, R, T and $\Delta G^{\ddagger}_{vis}$ are molar volume of the solvent, Avogadro number, Planck constant, Gas constant, temperature in K and free energy of activation for the viscous flow respectively ln ($\eta V/Nh$) plotted against T^{-1} yields a linear plot (Fig.5), with slope and

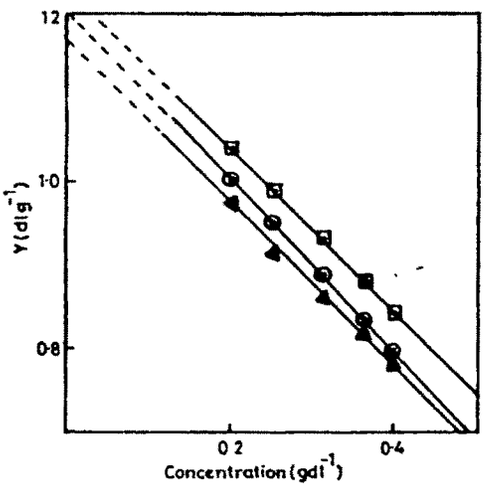

Fig.6 - Plot of Y vs concentration of PAA (g/dl) for ⊙-PAA - 0 05% CTAB. Δ-PAA-0.01% CTAB. ⊡-PAA - 0 1% CTAB where $Y = (\eta_r^{0.5} - 1/C(1.35\ \eta_r^{0.5} - 0.1)$

intercept giving $\Delta H^{\ddagger}_{vis}$ and $\Delta S^{\ddagger}_{vis}$ respectively. On plotting $\Delta H^{\ddagger}_{vis}$ and $\Delta S^{\ddagger}_{vis}$ against polymer concentration and extrapolating to C = 0, $\Delta H^{\ddagger o}_{vis}$ and $\Delta S^{\ddagger o}_{vis}$ values were obtained and hence $\Delta G^{\ddagger o}_{vis}$, was computed at any given temperature. The values seem to be almost independent of surfactant concentration. These values are 30.9 ± 0.2 at 35°C and 18.5 ± 0.9 kJ mol^{-1} for $\Delta G^{\ddagger o}_{vis}$ and $\Delta H^{\ddagger o}_{vis}$ respectively. The value of $\Delta S^{\ddagger o}_{vis}$ is equal to -39.7±2.3 J mol^{-1} K^{-1}. This $\Delta H^{\ddagger o}_{vis}$ is somewhat close to 17 kJ mol^{-1} - a characteristic value of spherocolloids[22].

The relative viscosity data at different concentrations were used for the calculations of voluminosity (V_E) of polymer solutions, at a given temperature in presence of CTAB. V_E was obtained by[10,21] plotting Y against concentration C(g dl^{-1}) where

$$Y = (\eta_r^{0.5} - 1)/C(1.35\ \eta_r^{0.5} - 0.1)$$

The straight line thus obtained was extrapolated to C = 0 and intercept yielded V_E (Fig.6). V_E at 35°C is shown in Table 3. The shape factor[10,21] was then calculated from the equation.

$$[\eta] = \nu.V_E$$

The shape factor gives us an idea about polymer molecules in solution. Values of shape factor (Table 3) are ~2.7 indicating very minor variation from spherical conformation of macromolecules in the presence of the surfactant[23]. In computing the shape factor and viscosity it was assumed that the polymer-surfactant system is nothing but a polymer system where an additive surfactant is present. That is the effect of the presence of CTAB on the polymer structure could be obtained.

Polyacrylamide-CTAB system in aqueous solution was studied at various temperatures by surface tension, conductance and viscosity. It was observed that CTAB interacts with the polyacrylamide. the interaction is in general mildly exothermic. The system shows higher intrinsic viscosity indicating interaction. The shape of polyacrylamide molecule in solution does not seem to change such in the presence of surfactants The PAA is somewhat surface active and also does not contain large hydrophilic group. However, the magnitude of thermodynamic quantities indicate mild interaction.

Acknowledgement

Thanks are due to the Inter University Consortium-Department of Atomic Energy Facilities, Indore, for financial assistance.

References

1 Saito S. *Nonionic surfactants - Physical chemistry*. Chapter 15. p 881. edited by M J Schick (Marcel-Dekker Inc New York) 1989.

2 Goddard E D, *Interaction of surfactants with polymers and proteins*, edited by E D Goddard & K P Ananthpadmanabhan (CRC press, Boca Raton, FL) 1993. p 123

3 Goddard ED, *Colloids Surf*. 19 (1986) 255.

4 Cabane B & Duplessix R, *J Phys (Paris)* 48 (1987) 651

5 Chari K, Antalek B, Lin M Y & Sinha S K, *J chem Phys*. 7 (1994) 100

6 Biggs S, Selb J & Candau F, *Langmuir*. 8 (1992) 838

7 Hoffmann H & Huber G, *Colloids Surf*. 40 (1989) 181

8 Zana R, Binana-Limbeli W, Kamenka N & Lindman B, *J phys Chem*. 96 (1992) 5461

9 Bloor D M, Mwakibete H K O & Wyn-Jones E, *J colloid interface Sci*. 178 (1996) 334.

10 Rangaraj A, Vangani V & Rakshit A K, *J appl polym Sci*. 66 (1997) 45.

11 CMC values obtained by different methods are different. Conductivity method gives a value of 0 90 mM Please see Moulik S P, Haque Md E, Jana P K & Das A R *J phys Chem*. 100 (1996) 701

12 Minatti E & Zanette D, *Colloids Surf*. 113 (1996) 237

13 Cabane B & Duplessix R, *J Phys (Paris)*, 43 (1982) 1529

14 Romsted L S, Ph D Thesis Indiana University, Bloomington, IN, 1975 (Please see Zanette D, Ruzza A A, Frochner S J & Minatti E, *Colloids Surf*. 108 (1996) 91

15 Zana R, Lang J & Lianos P, *Polym Prepr Am chem Soc Div Polym Chem*, 23 (1982) 39

16 Verral R E, Milioto Z & Zana R, *J phys Chem*, 92 (1988) 3939.

17 Sharma B G & Rakshit A K, *J Colloid Interface Sci*, 129 (1989) 139.

18 Koshy L & Rakshit A K, *Bull chem soc Japan*, 64 (1991) 2610.

19 Sulthana S B, Bhat S G T & Rakshit A K, *Colloids surf*, 111 (1996) 57

20 Sulthana S B, Bhat S G T & Rakshit A K, *Langmuir*, 13 (1997) 4562

21 Vangani V & Rakshit A K, *J appl polym Sci*, 60 (1996) 1005.

22 Prarsad Ch D & Singh H N, *Colloid Surf*, 59 (1991) 27

23 Kohler H H & Strand J, *J phys Chem*, 94 (1990) 7628